Pergamon

Cement and Concrete Research 31 (2001) 633–639

CEMENT AND CONCRETE RESEARCH

The effects of limestone characteristics and calcination temperature to the reactivity of the quicklime

Antonia Moropoulou*, Asterios Bakolas, Eleni Aggelakopoulou

Department of Chemical Engineering, Materials Science and Engineering Sector, National Technical University of Athens, Iroon Polytechniou 9, Athens 15780, Greece

Received 7 August 2000; accepted 6 December 2000

Abstract

This study has examined the effects of limestone characteristics (microstructure and texture) and calcination temperature on the reactivity of the produced quicklime. Two types of limestone have been calcined at four selected temperatures (900°C, 1000°C, 1100°C, 1200°C), and the produced quicklime was slaked. Chemical, physical, and mineralogical analyses have been performed in limestone, quicklime, and slaked lime samples with the intention of studying the quicklime reactivity. Test results indicate that the lower the limestone calcination temperature, the more reactive the produced quicklime. The optimum calcination temperature is ~900°C, which was the temperature performed in traditional limekilns. Concerning the quicklime, the reactivity is related to its microstructure, which is, in turn, related to microstructural characteristics of the limestone (texture, grain size, porosity). The most reliable factors for the estimation of quicklime reactivity are the specific surface area of the quicklime and the rate of temperature increase during the slaking process.

Keywords: $Ca(CO_3)_2$; CaO; Microstructure; $Ca(OH)_2$; Quicklime reactivity

1. Introduction

Lime has been used as an essential binder for the production of mortars and plasters since 7000 BC [1]. Greeks and Romans were familiar with the use of lime and they used it either as pure binder in order to get aerial mortar or mixed with pozzolana (natural or artificial) for the manufacture of hydraulic mortars. Lime mortars have been used for masonry structures as joint mortars, as supporting or decorative materials (pavements, mosaics, frescoes), and even as binders for waterproof linings (cisterns, reservoirs, baths). Through the centuries, lime mortars have been proven to be well compatible to the historic building materials and longlasting under severe mechanical and environmental loads [2].

By the middle of the 19th century, the process of lime production changed. By using oil, gas, and carbon dust as fuel in limekilns, the dissociation temperature was exceeded and the produced lime was overburnt [3]. Therefore, the current lime mortars are different from the historic ones and consequently manifest behaviour incompatible to the structural materials on the mason-dry scale.

Besides lime, negative results have also been observed in using cement or polymers as restoration mortars since these are too hard, brittle, and impervious for historic masonries [4,5]. Hence, the architectural conservation community has recently paid attention to the scientific study of traditional lime mortars.

In the literature, there are several references concerning factors that may affect the quality of quicklime and slaked lime. Generally, these factors are characteristics of the limestone, calcination temperature, pressure acquired in kilns, rate of calcination, and fuel quality [6,7]. Nevertheless, no studies have been reported, to the best of our knowledge, about the specific effect(s) of the various factors (raw materials, calcination temperature) to the reactivity of the produced quicklime. Hence, in this study, in order to specify these effects, the investigation of the microstructural characteristics of the produced quicklime has to be performed properly.

* Corresponding author. Tel.: +30-1-772-3276; fax: +30-1-772-3215.
E-mail address: amoropul@central.ntua.gr (A. Moropoulou).

0008-8846/00/$ – see front matter
PII: S0008-8846(00)00490-7

2. Experimental

2.1. Materials and procedure

The raw materials used in the production of lime were two Cretan quarry limestones, Sises (L_S) and Latzima (L_L), from Greece. These limestones were selected in order to evaluate the characteristics of Cretan quicklime, which is the most commonly used binder in restoration mortars in Crete.

Limestones present macroscopically different characteristics. L_S is a light-coloured grey limestone with hardly distinguished crystals, whereas L_L is a dark grey limestone comprised of indiscriminate, tiny crystals. Microcracks have occurred throughout the mass of both limestones due to the quarrying process or to the formation process of limestone.

Samples of limestones were calcined at four different temperatures (900°C, 1000°C, 1100°C, 1200°C) for 24 h for the production of quicklime. The quicklime was hydrated, with the addition of appropriate amount of water until slaked lime putty with adequate consistency was produced. The temperature increase rate during the slaking process was estimated. The evaluation of the quicklime and slaked lime microstructural characteristics has been performed.

The production procedure is presented in Fig. 1. Table 1 shows the types of limestone, quicklime, and slaked lime with their abbreviated codes.

Table 1
Abbreviation codes of testing materials (limestone, quicklime, slaked lime)

Quarry	L	T_c (°C)	Q	S
Sises	L_S	900	Q_{S9}	S_{S9}
		1000	Q_{S10}	S_{S10}
		1100	Q_{S11}	S_{S11}
		1200	Q_{S12}	S_{S12}
Latzima	L_L	900	Q_{L9}	S_{L9}
		1000	Q_{L10}	S_{L10}
		1100	Q_{L11}	S_{L11}
		1200	Q_{L12}	S_{L12}

L, limestone; T_c, calcination temperature of limestone; Q, quicklime; S, slaked lime.

2.2. Analytical methods and techniques

Analyses were performed in limestone, quicklime, and slaked lime samples by using the following analytical procedures.

- X-ray diffraction (XRD) analysis of finely pulverized limestone samples for the identification of the presented crystalline compounds. The analyses were performed with a Siemens D-5000 (with a graphite crystal monochromator and a Cu anticathode). The diffraction interval was between $2\theta - 5°$ and $2\theta - 50°$ with a step of 0.02°.
- Transmitted light microscopy (Nikon, Optiphot-Pol) was carried out in polished thin sections of the limestone in order to identify the texture, shape, and size of the grains.
- Calcimetry (gas volumetric method, Dietrich Fruhking) has been accomplished in pulverized limestone to determine the CO_2 content.
- Atomic absorption spectroscopy (AAS, Perkin Elmer 3300) was used on limestone to determine the percentage of ions, calcium (Ca^{2+}), and magnesium (Mg^{2+}).
- Differential thermal and thermogravimetric analyses (simultaneous DTA/TG) were carried out to determine quantitatively and qualitatively the various compounds presented in the samples. Analyses were performed in samples of limestone and lime putty in static air atmosphere at a temperature range of 30–1000°C and a gradient of 10°C/min (Netzsch 409 EP DTA/TG).
- Mercury intrusion porosimetry (Fisons, Porosimeter 2000) was used to measure the microstructural characteristics of limestone, quicklime, and solid lime putty. The estimation of total porosity, specific surface area, pore radius average, total cumulative volume, and apparent density was accomplished.
- Adsorption of nitrogen was performed on quicklime and lime putty in order to evaluate the value of specific surface area by physical sorption isotherm data according to the method of Brunauer–Emmet–Teller (BET). The above values are compared with the ones obtained from the mercury intrusion porosimetry.

3. Results and discussion

3.1. Limestone characteristics

Microphotographs of limestones ($\times 50$) by transmitted light microscopy are illustrated in Fig. 2. As shown, limestone L_S exhibited small to large size grains, which are distributed inhomogenously throughout the mass. On the other hand, limestone L_L presented fine grains and a homogenous texture.

The mineralogical composition of limestone was obtained by XRD analysis. The main component proved to be calcite for both samples, although this does not preclude the possibility of the presence of small quantities ($<5\%$) of other polymorphs of $CaCO_3$ and dolomite.

Table 2 reports the results of chemical analyses performed by calcimetry, DTA/TG, and AAS. The weight loss

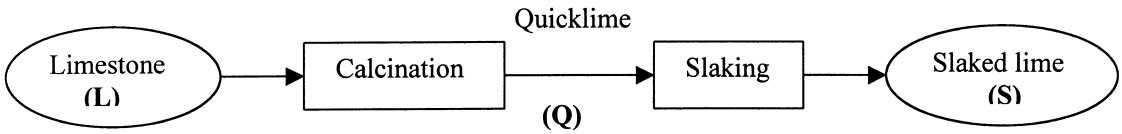

Fig. 1. The production procedure of slaked lime.

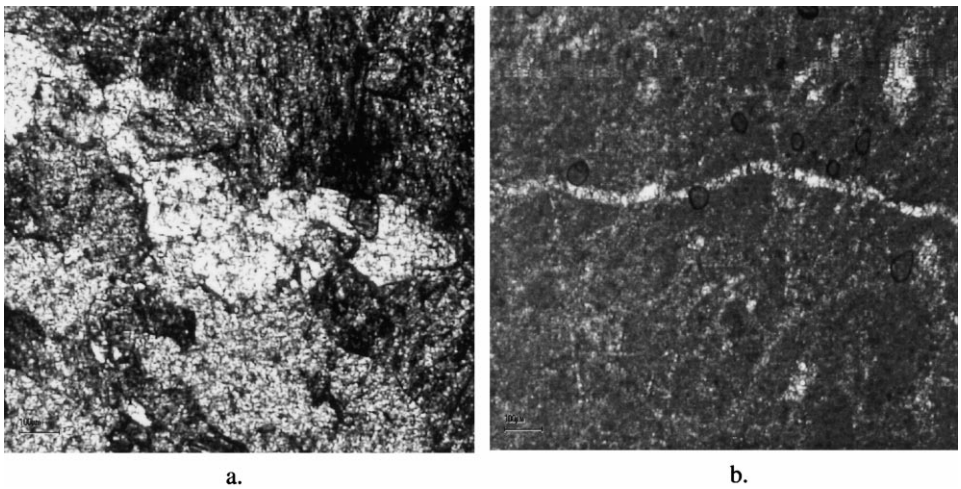

Fig. 2. Microphotographs of limestones (a) L_S (× 50), (b) L_L (× 50).

above 600°C, measured by TG, is attributed to the CO_2 from the decomposition of calcium carbonate [8]. Comparing the percentage values of CO_2 measured by calcimetry and DTA/TG, it is evident that the values are very high and similar to each other. Thus, both limestones could be characterised as high-calcium ones. Furthermore, it is observed that the percentage of CO_2 for both limestones is higher than the theoretical one. This fact might be ascribed to the presence of a small amount of dolomite in the limestone. The content of ions Ca^{2+} and Mg^{2+} is evaluated by using AAS analysis [9]. The results are reported in Table 2. The relative content of carbonate compounds (according to Ca^{2+}, Mg^{2+} content) is analogous to that attained by calcimetry and TG. Furthermore, L_L has revealed higher percentage of Mg^{2+} than L_S, which may be ascribed to its higher dolomite content. Thus, from the chemical analyses, it can be concluded that both limestones presented identical chemical composition, with a percentage of calcite compounds greater than 99%, and that small amount of dolomite is presented only in L_L.

Microstructural data by mercury intrusion porosimetry are reported in Table 3 and expressed as C_v (total cumulative volume), $P_{\%}$ (percentage total porosity), R_m (average pore radius), γ (apparent density), A_s (specific surface area). Both limestones indicated low values in total cumulative volume, total porosity (lower than 1%), pore radius average, and specific surface area. The value of apparent density was found to be characteristic for a limestone. Comparing the two limestones, L_S demonstrated higher values in total cumulative volume, total porosity, and pore radius average. Thus, L_L might be characterised as a more compact and harder limestone than L_S.

Pore size distributions of the two examined limestones are presented in Figs. 3 and 4. L_S indicated a smooth pore size distribution with pore radius from 0.03 to 10 μm with an average of 0.14 μm. Two areas can be noticed in the pore size distribution of L_L. In the first one, pore radii are between 0.003 and 0.01 μm and in the second one, pore radii are in the range of 0.05–10 μm.

3.2. Calcination of limestone

The evaluation of the dissociation completion was performed by measuring the mass loss of the samples before and after calcination. The mass loss corresponds to the released amount of CO_2 during the calcination process. The results are considered satisfactory and in accordance with the data obtained by TG and calcimetry analyses. The measured percentage of mass loss is around 44%. Therefore, the dissociation of limestone and the production of quicklime are successfully accomplished.

Table 4 presents the microstructural characteristics of produced quicklime evaluated by mercury intrusion porosimetry and nitrogen adsorption. It can be observed that for both samples, total cumulative volume, total porosity, and specific surface area decrease as the calcination tempera-

Table 2
Chemical analyses data of limestones

	Cc	DTA/TG	AAS			
L	Mass loss CO_2 (%)		Ca^{2+} (%)	Mg^{2+} (%)	CaO (%)	MgO (%)
L_S	43.27	44.28	39.68	0.20	55.55	0.33
L_L	44.46	44.33	39.20	0.50	54.88	0.83

DTA/TG, differential thermal and thermogravimetric analyses; AAS, atomic absorption spectroscopy; Cc, calcimetry (gas volumetric method).

Table 3
Porosimetric data of limestones

L	C_v (mm^3/g)	γ (g/cm^3)	$P_{\%}$ (%)	R_m (μm)	A_s (m^2/g)
L_S	2.6	2.70	0.7	0.14	0.02
L_L	1.0	2.71	0.3	0.01	0.17

C_v, total cumulative volume (mm^3/g); γ, bulk density (g/cm^3); $P_{\%}$, total porosity (%); R_m, pore radius average (μm); A_s, specific surface area (m^2/g).

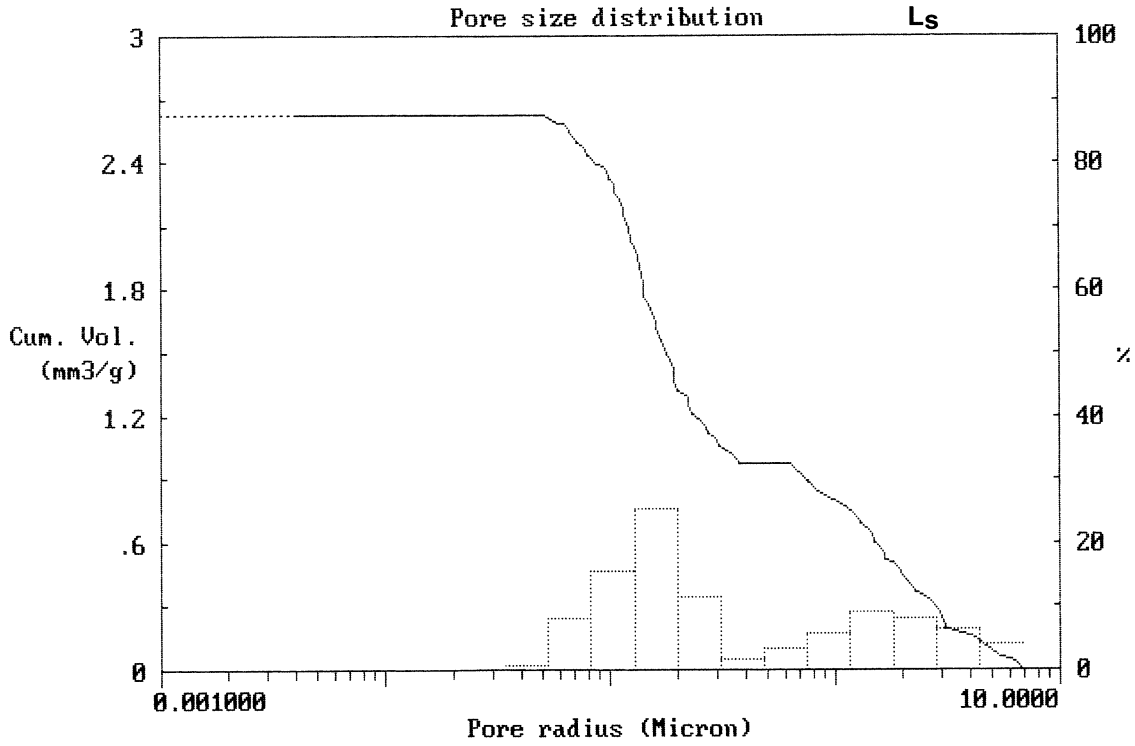

Fig. 3. Pore size distribution of L_S.

ture rises, whereas the values of apparent density and pore radius average increase. The values of specific surface area measured by nitrogen adsorption are slightly increased in relation to the porosimetric ones. The upper increase can be attributed to the nitrogen adsorption capability to measure smaller pores. The value of specific surface area becomes maximum for Q_S and for the calcination temperature of 900°C.

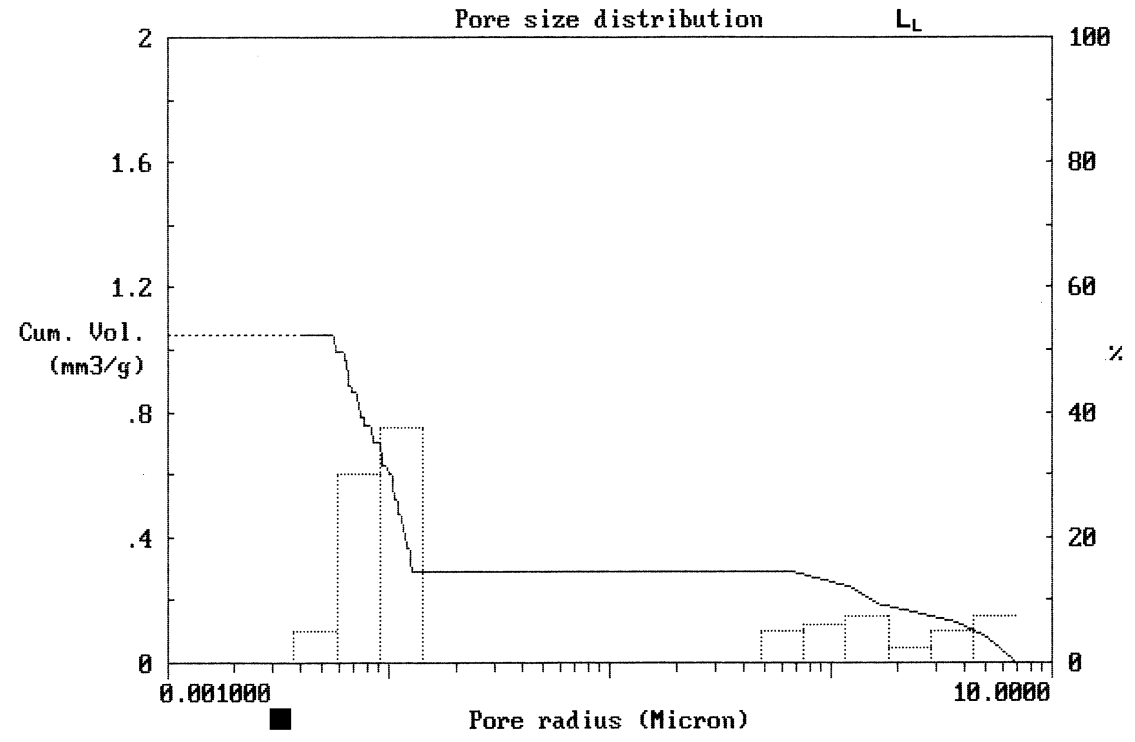

Fig. 4. Pore size distribution of L_L.

Table 4
Microstructural characteristics of quicklime

Q	C_v (mm^3/g)	γ (g/cm^3)	$P_{\%}$ (%)	R_m (μm)	A_s (m^2/g)	A_s, BET (m^2/g)
Q_{S9}	342.5	1.64	56.2	0.09	5.30	5.33
Q_{S10}	306.3	1.74	53.3	0.11	3.47	3.60
Q_{S11}	262.5	2.03	53.3	0.29	1.18	2.28
Q_{S12}	174.8	2.49	43.5	0.33	0.49	1.17
Q_{L9}	321.5	1.67	53.7	0.18	3.19	3.85
Q_{L10}	261.4	1.82	47.6	0.24	1.97	2.16
Q_{L11}	146.4	2.23	32.6	0.43	0.87	1.44
Q_{L12}	74.0	2.61	19.6	0.54	0.31	0.66

Comparing the two samples, Q_S presents higher values in total cumulative volume, total porosity, and specific surface area than Q_L. Hence, the limestone and quicklime microstructure and texture can be related. Limestone L_S exhibits a rather porous structure, and after calcination, the produced quicklime seems to maintain this structure, presenting high values in porosity, total cumulative volume, and specific surface area. On the other side, limestone L_L, which is a hard and compact limestone with low porosity, produces quicklime with denser structure, lower porosity, lower specific surface area, and higher pore radius average after calcination than L_S. In addition, observing the values of apparent density and total cumulative volume for the samples, it is evident that limestone L_L presents higher volume contraction than L_S during calcination.

Figs. 5 and 6 present the pore size distribution overlay for Q_S and Q_L, respectively, produced at 900°C and 1200°C. It is observed that with increase of calcination temperature, the pore radii are shifted to larger pores with elimination of smaller pores due to the coalescence phenomenon occurring during calcination [7]. Q_L exhibits greater decrease of total cumulative volume and smaller pore radii (<7.5 μm) than Q_S. On the other hand, Q_S presents macropore structure with pore radii in the range of 0.07–50 μm.

3.3. Hydration of quicklime

During the hydration of quicklime, two simultaneous phenomena are observed: the temperature increases (exothermic reaction) and the volume of the paste is expanded. In this study, the hydration of quicklime took place in a heat-insulating vessel with gradual addition of water. The vessel was equipped with a stir, a thermometer, and a timer in order to estimate the temperature increase. The rate of temperature increase is defined as the ratio of temperature vs. time. The results are reported in Table 5. Observing the data (Table 5), it is clear that the lower calcination temperature increases the value of rate of temperature increase. The most reactive quicklime is obtained by calcination of L_S and for a calcination temperature of 900°C. Traditional limekilns, using wood and charcoal as fuel, acquired this range of temperature (850–900°C) and it seems to be the primary reason of producing high-quality lime.

Bearing in mind the values of the specific surface area of quicklime (Table 4), it is assumed that there is a relation between the rate of temperature increase and the specific surface area. The larger the specific surface area, the higher

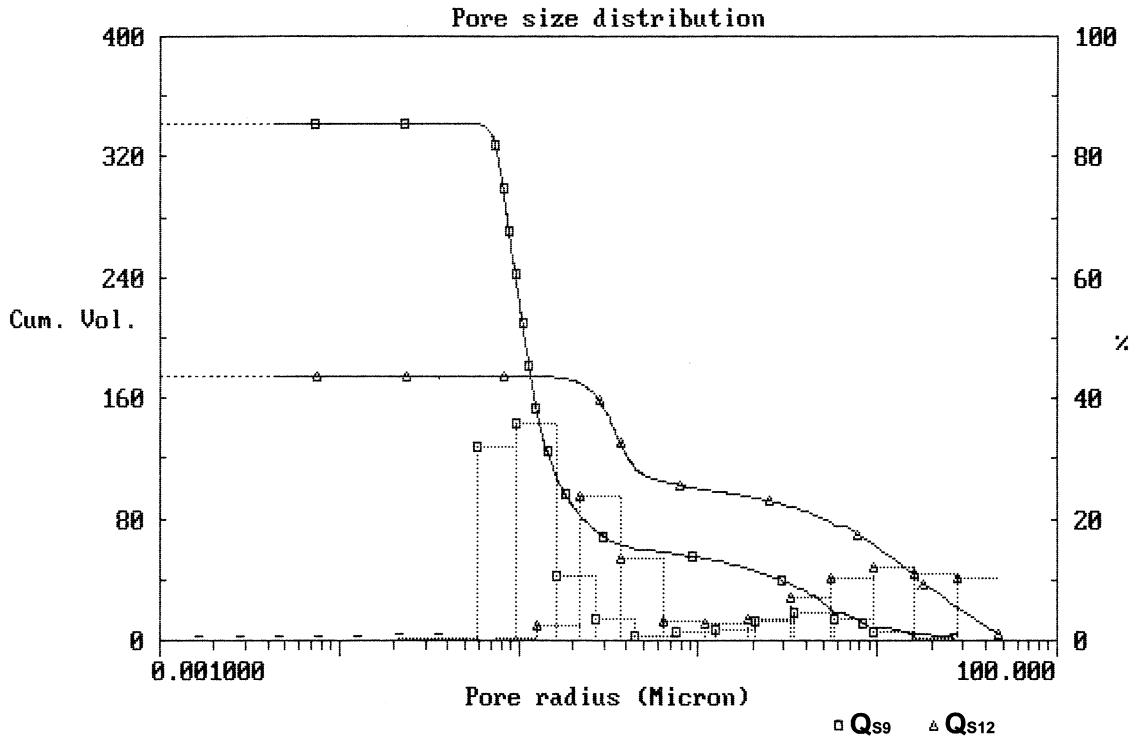

Fig. 5. Pore size distribution of Q_S.

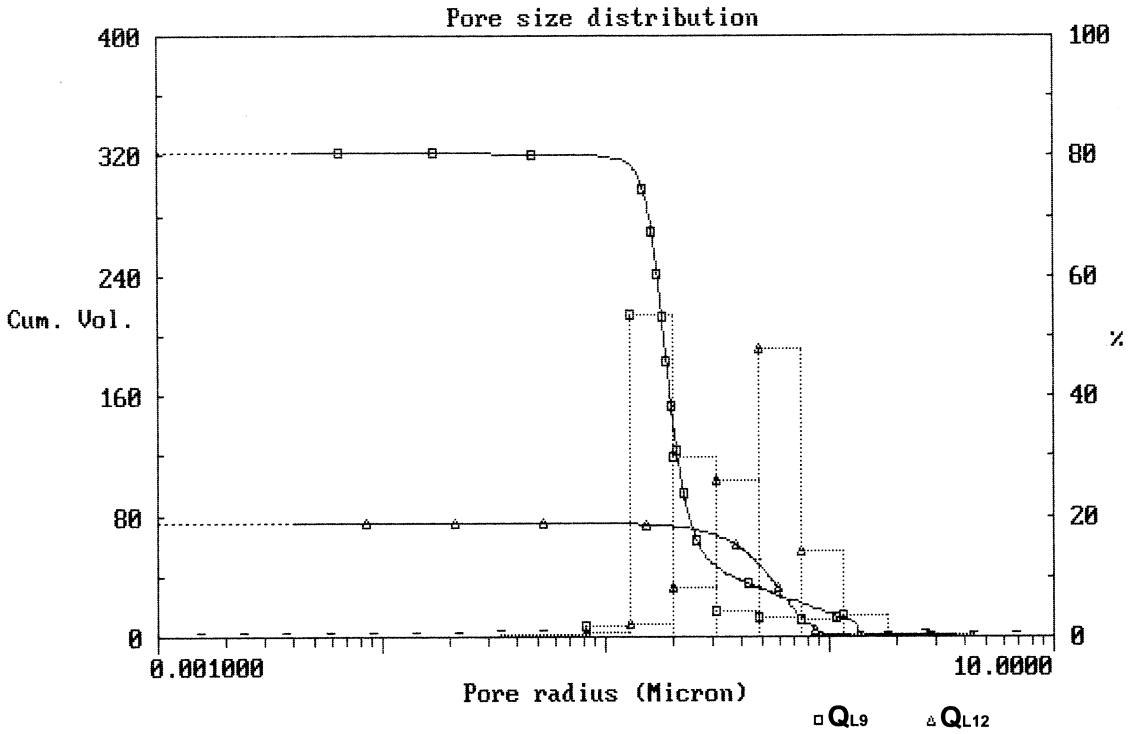

Fig. 6. Pore size distribution of Q_L.

the rate of temperature increase, and so the quicklime is more reactive. Thus, the assumption that surface area might be a reliable factor for the estimation of quicklime reactivity appears to be confirmed.

The process of slaking can easily be monitored by measuring the $Ca(OH)_2$ content in the slaked lime powder. Therefore, lime putty was dried out in a furnace and DTA/TG was performed in samples of lime powder in order to estimate the $Ca(OH)_2$ content. Since this content was greater than 96% for all samples, it could be assumed that the slaking of quicklime had been completed. In addition, a small amount of $CaCO_3$ (about 1%) was detected, which could be ascribed to the process of carbonation that took place.

The estimation of microstructural characteristics was carried out using mercury intrusion porosimetry and nitrogen adsorption. The microstructural data are reported in Table 6. In general, increasing the limestone calcination temperature decreases total cumulative volume, total porosity, and specific surface area. S_S indicates higher values in specific surface area than S_L, obtaining its maximum value at a calcination temperature of 900°C.

Table 5
Results of quicklime hydration

Q	T_{max} (°C)	Δt (s)	RTI (°C/s)
Q_{S9}	176	100	1.76
Q_{S10}	164	110	1.49
Q_{S11}	158	180	0.88
Q_{S12}	147	180	0.82
Q_{L9}	170	150	1.13
Q_{L10}	157	170	0.92
Q_{L11}	148	170	0.87
Q_{L12}	142	220	0.64

T_{max}, the maximum value of temperature (°C); Δt, the required time interval for the acquisition of T_{max}; RTI: rate of temperature increase (ratio of T_{max} vs. Δt).

4. Conclusions

This study has investigated the effect of limestone characteristics and calcination temperature to quicklime reactivity. The following conclusions can be drawn based on the experimental results.

- Quicklime produced by calcination of limestone L_S was more reactive than that produced by L_L. L_S exhibits small to large size of crystals, an inhomogeneous distribution throughout the mass, and a less compact structure than L_L. It can be characterised as high-calcium limestone with low content of impurities. Further investigation should be accomplished regarding the effect of limestone texture to quicklime reactivity.

Table 6
Microstructural characteristics of lime putty

S	C_v (mm^3/g)	γ (g/cm^3)	$P_{\%}$ (%)	R_m (μm)	A_s (m^2/g)	A_s, BET (m^2/g)
S_{S9}	685.1	0.95	65.1	0.07	25.01	22.96
S_{S12}	583.8	1.01	58.0	0.10	20.18	19.20
S_{L9}	733.5	0.87	63.8	0.89	8.76	9.73
S_{L12}	683.4	1.02	69.7	0.63	6.11	7.11

• From the results obtained, it is obvious that the lower the calcination temperature, the higher the specific surface area and the more reactive the quicklime. The greatest surface area was obtained for limestone calcined at 900°C, which was the temperature performed in traditional limekilns. High calcination temperatures acquired in modern limekilns are the major reason for the production of low-quality lime.

• The specific surface area can be a reliable factor for the estimation of quicklime reactivity. The greater the specific surface area, the more reactive the quicklime.

• The rate of temperature increase may be an additional parameter for the evaluation of quicklime reactivity which is augmented by increasing the quicklime reactivity.

• Further investigations should be performed to evaluate the rendering (R) of quicklime during the slaking as a parameter of the slaked lime quality and to search for the relation among rendering, quicklime specific surface area, and reactivity.

References

[1] R. Malinowsky, Y. Grafinkel, Prehistory of concrete, Concr. Int., (1991) 62–68.

[2] A. Moropoulou, P. Maravelaki-Kalaitzaki, M. Borboudakis, A. Michailidis, P. Michailidis, M. Chronopoulos, Historic mortars technologies in Crete and guidelines for compatible restoration mortars, PACT: Revue du groupe europeen d'etudes pour les techniques physiques, chimiques, biologiques et mathematiques appliquees a l'archeologie 55 (1998) 55–72.

[3] M. Wingate, Small-Scale Lime Burning: A Practical Introduction, Intermediate Technology Publications, London, 1985.

[4] S. Fassina, The Effects of Past Treatments on the Acceleration of Weathering Processes in the Statues of Prato Della Valle, Intern. UNESCO-RILEM Congress on the Conservation of Stone and other Materials, Paris, 1993, Proceedings, p. 129.

[5] Th. Skoulikidis, Critique on the Old Materials of Consolidation and Protection for Monuments Surfaces, Special Edition of NTUA, Athens, 1998.

[6] G. Gallo, Sulla Strutura dei Calcari per Calce Grassa, Ann. Chim. Appl., (1915) 214–225.

[7] R.S. Boynton, The Chemistry and Technology of Lime and Limestone, 2nd ed., Wiley, New York, 1980.

[8] R.C. Mackenzie, Differential Thermal Analysis 2, 1st ed., Academic Press, London, 1970.

[9] P. Robinson, Determination of calcium, magnesium, manganese, strodium, sodium and iron in the carbonate fraction of limestones and dolomites, Chem. Geol. 28 (1980) 135–146.